J. Synchrotron Rad. (1999). **6**, 403–405

Time-resolved energy-dispersive XAS studies of photoinduced electron transfer intermediates in electron donor–acceptor complexes

Lin X. Chen*, Peter L. Lee†, David Gosztola*, Walter A. Svec*, and Michael R. Wasielewski*§

**Chemistry Division, Argonne National Laboratory, Argonne, IL 60439-4831*
†Experimental Facilities Division, Argonne National Laboratory, Argonne, IL 60439-4831
§Department of Chemistry, Northwestern University, Evanston, IL 60208-3113
e-mail: lchen@anlchm.chm.anl.gov
Fax: (630)-252-9289

The structure around the Fe atom of a photoinduced electron transfer intermediate in a di-porphyrin electron donor/acceptor complex is studied with time-resolved energy dispersive X-ray absorption spectroscopy. Photoinduced electron transfer from the lowest excited triplet state of a Zn porphyrin attached at a fixed 25 D distance by means of a long spacer molecule to an Fe(III) porphyrin occurs with a 6 ms time constant at 77 K. Time domain X-ray absorption measurements show that Fe(III) is transiently photoreduced to Fe(II) and that the bond between the Fe atom and a pyridine molecule ligated to it weakens substantially upon reduction of the Fe. Coupling of ligand loss to reduction of Fe(III) to Fe(II) provides a mean of stabilizing the reduced intermediate.

KEYWORDS: energy dispersive XAS, photoinduced electron transfer, XANES, time-resolved XAFS, porphyrin complexes

1. Introduction

Photoinduced electron transfer (ET) reactions are important biological and chemical processes. The rates of these reactions are affected by the coupling of the electron motion to nuclear motions within the electron donor and acceptor molecules as well as to those molecules in the surrounding environment (Barbara et al., 1996). However, the charge separate intermediates in most photoinduced ET reactions have lifetimes that are too short for steady-state X-ray structure determination. Thus far, the structures for the intermediates from photoinduced ET have only been obtained using matrix isolation at low temperatures and studied with steady-state X-ray methods (Chance et al., 1983; Powers et al., 1984; Chen et al., 1993, 1994, 1995). Recently, time-resolved X-ray techniques were used to capture the photogenerated intermediates on short time scales (Perman et al., 1998; Thiel et al., 1993). Photoinduced ET reactions have been studied extensively in hybrid hemoglobins in which one Fe(III) porphyrin (Fe(III)P) is replaced by a Zn or Mg porphyrin (ZnP or MgP) (Nocek et al., 1997; Natan et al., 1991). Photoexcitation of ZnP or MgP produces the lowest excited triplet state, ^{3}ZnP or ^{3}MgP, respectively, which donates an electron to a distant Fe(III)P. Many of these photoinduced ET reactions in heme proteins occur on a millisecond time scale (Natan et al., 1991). Thus, the reaction intermediate structures may be studied with currently available time-domain energy dispersive X-ray absorption spectroscopy (EDXAS) (Fontaine et al., 1992; Lee et al., 1996). In this study, we used EDXAS at Fe K-edge with 5-ms time resolution to directly probe structural changes around Fe in Fe(III)P in an electron donor/acceptor complex **2** (Figure 1), which undergoes a photoinduced ET reaction: ^{3}ZnP-L-spacer-Fe(III)P-L → ZnP$^+$-L-spacer-Fe(II)P-L, where L = ligand, acetate (OAc) or pyridine (py). $^{1\text{ or }3}$ZnP is the optically excited singlet or triplet state, and ZnP$^+$ is the photogenerated cation.

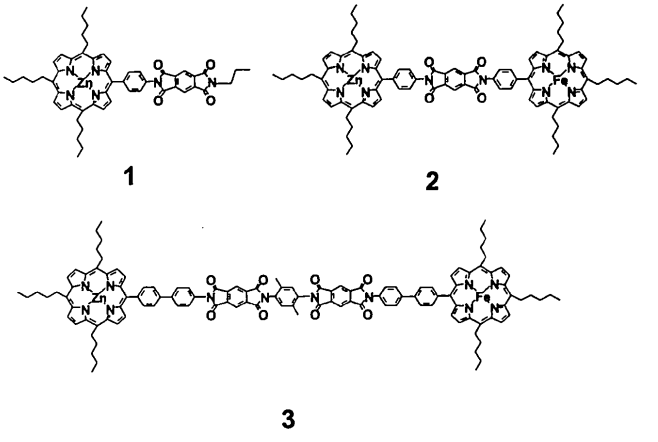

Figure 1
Molecular structures of compounds **1-3**.

2. Experimental

1-3 were synthesized based on procedures given elsewhere (Wiederrecht et al., 1996). **1** with no electron acceptor Fe(III)P is used as a reference compound. The Zn - Fe distance in **2** is 25 Å, while that in **3** is 45 Å. The samples were dissolved in 2-methyltetrahydrofuran (MTHF) without or with 1-2 % pyridine. The optical transient absorption experiments were conducted on **1-3** at 77 K using 425 nm, 4 ns laser excitation pulses, and monitoring the concentration of ^{3}ZnP at 475 nm[22], and the ground state recovery kinetics at 560 nm from a xenon flash lamp probe.

EDXAS measurements were carried out at Beamline X6A, National Synchrotron Light Source (NSLS), Brookhaven National Laboratory. The configuration of the beamline has been described elsewhere (Lee et al., 1996). The time resolution of the apparatus is 5 ms limited by the linear diode array detector read-out time. Photoexcitation of ZnP at 563 nm was provided by 6-ns laser pulses from a Nd:YAG pumped OPO (optical parametric oscillator) at a 10 Hz repetition rate at 30 mJ/pulse. The laser pulses were synchronized with the detector read-out. 2000 spectra were averaged for each 5-ms duration. Two identical sample compartments were constructed on the same sample holder, one for the sample and the other for the blank MTHF solvent as the reference. The sample compartment has a 3-mm thickness in the X-ray path defined by two parallel Mylar windows. A rectangle quartz slab of 3-mm wide was sandwiched between the two Mylar windows and was aligned with one of the edges of the Mylar windows (see Figure 2). The X-ray beam is parallel to the quartz surface and can be positioned very close to the surface (e.g., 0.2 mm). Thus, the distance that the laser light needs to travel from the quartz surface to the sample where the X-ray hits is about 0.2

mm. This configuration with a 3-mm X-ray path and a 0.2 mm laser light path partially compensates the discrepancy between the absorption coefficients of the sample for the X-ray and for the laser light. Therefore, measurements of XANES spectra at 7.1 KeV for a sample with only 2×10^{-3} M concentration using the transmission

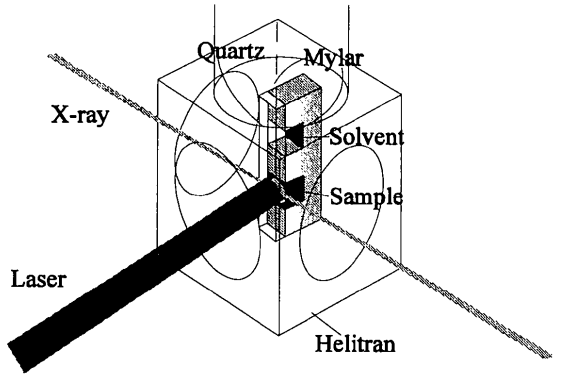

Figure 2.
The sample cell and experimental setup

geometry became feasible. The sample was irradiated at 70K in a MTHF matrix inside a cryostat by the laser at a right angle with respect to the X-ray beam (see Figure 2). Nearly 100% of **2** was excited according to a calculation with considerations of the laser pulse energy, sample geometry, concentration (both ZnP and FeP absorb at 563 nm, but the latter decays to the ground state on a picosecond time scale) and optical absorption coefficient at 563 nm before the XANES experiments. The excited ZnP in **2** undergoes intersystem crossing with a quantum yield of about 0.8 which would be the maximum ET yield. In this particular ET system, the optical spectroscopy is not able to obtain the ET yield because of the spectral overlap of different species. The XANES appears to be a way to obtain this information.

3. Results and Discussion

To establish the kinetics for the photoinduced ET processes in **1-3**, optical transient absorption measurements were performed before the EDXAS measurements. The time constants for the triplet state decay and the ground state recovery at 77 K are listed in Table 1. At 77 K, ZnP and **1** have triplet state decay time constants of about 18-20 ms. **2** and **3** with acetate ligands on Zn and Fe exhibit almost the same decay time constants, 16-18 ms. However, adding pyridine ligands to the metals in **1-3** shortens the decay time constant of ^{3}ZnP within **2** to 6 ms, while those in **1** and **3** remained unchanged. The same trend was observed in the ground state recovery time constants. The shortened lifetime of ^{3}ZnP within **2** with pyridine ligands suggest that a new triplet quenching mechanism occurs when **2** is ligated with pyridine. Three possible quenching mechanisms for ^{3}ZnP-py in **2** were: (a) ET from ^{3}ZnP-py to Fe(III)-py, forming ZnP^+-py and Fe(II)P-py; (b) energy transfer from ^{3}ZnP-py to Fe(III)P-py, and (c) quenching of ^{3}ZnP in ^{3}ZnP-py by the pyridine ligand. (c) was eliminated because the triplet state decay kinetics of **3** (with a donor-acceptor distance of 45 Å) were unchanged by ligation of Fe and Zn with pyridine. The triplet decay time constants for **2** and **3** with acetate ligands are almost the same as that for **1**, indicating that energy transfer from ^{3}ZnP to Fe(III)P is very inefficient and does not contribute to the decay of ^{3}ZnP. Ligation of Fe(III)P with pyridine in both **2** and **3** makes the free energy of reaction for ET more favorable by about 0.5 eV. However, the quenching of ^{3}ZnP-py in **2** only suggests that (a) is the most plausible mechanism. Adding a pyridine ligand to the Fe in **3** does not affect the triplet state decay rate in **3**, because the donor-acceptor distance in **3** is too long to establish an effective electronic coupling for the ET to occur. The above results strongly suggest that the quenching of ^{3}ZnP when pyridine ligates Zn and Fe in **2** is most likely due to ET from ^{3}ZnP-py to Fe(III)P-py with a 6 ms time constant. Since the ground state recovery data implies that back ET occurs with an 8 ms time constant (Table 1), the concentration of the transient Fe(II)P-py intermediate is sufficient for detection in the EDXAS experiment, which allows us to probe the structure in the vicinity of the Fe atom.

Table 1
Time constants for ZnP triplet state decay and ground state recovery at 77 K

Compound	Triplet state decay τ(ms) @475nm	Ground state recovery τ(ms) @560nm
ZnP (OAc or py)	20.3 ± 0.1	16.7 ± 0.1
1 + OAc or py	18.3 ± 0.1	17.7 ± 0.1
2 + OAc	17.8 ± 0.5	15.8 ± 0.2
2 + Py	5.6 ± 0.1	7.9 ± 0.2
3 + OAc	15.9 ± 0.1	14.2 ± 0.5
3 + Py	15.5 ± 0.1	19.0 ± 0.7

XANES spectra taken at the EDXAS beamline for **2** at the Fe K-edge (7.112 KeV) at different time delays following the laser excitation pulse are shown in Figure 3. The spectrum taken during 0-5 ms is very similar to the ground state **2** spectrum agreeing with the results from the transient absorption which indicate that during 0-5ms only very small fractions of Fe(III) in **2** would be reduced due to ET from ZnP to Fe(III)P. Using this spectrum as the reference for unreduced Fe(III), the clearest changes in the XANES spectra due to photoinduced ET occur at the pre-edge region and at the beginning of the transition edge. The largest change is at a time delay of 5-10 ms when the spectrum shows an apparent increase in the pre-edge feature (in the region of 3-8 eV) and a slight down-shift of the transition energy position at the beginning of the transition edge (in the region of 8-15 eV). Moreover, the position of the pre-edge features appeared to have shifted to an energy 2 - 2.5 eV higher than that of the ground state.

XANES spectra of the Fe atom in **2** reflect both its oxidation state and coordination geometry. This can be demonstrated by comparing XANES spectra of Fe(II) phthalocyanine and the ground state of **2** taken from a conventional XAFS beamline (X6A, NSLS) in Figure 3. The former has an Fe(II) in a square planar geometry and the latter, an Fe(III) in a square pyramidal geometry. The main changes in the XANES spectrum of the former from that of the latter are: (1) the down-shift of the transition edge position (see the region of 8-15eV), (2) an appearance of a sharp peak in the middle of the rising edge (at ~6.2eV), and (3) a reduction of a small pre-edge peak at 3eV. The first change is due to lower positive charges in the Fe(II) atom than in Fe(III), which results in less energy required to excite the 1s electron to the continuum. The second change comes from a

transition from the 1s orbital to an orbital with p_z character, most likely, $4p_z$, based on X-ray polarization dependence XAFS spectra of a series of $CuCl_4^{2-}$ and carboxymyoglobin (Smith et al., 1985; Bianconi et al., 1985; Catier et al., 1992). The third change is due to a molecular symmetry difference between the square planar (centrosymmetric) and square pyramidal (non-centrosymmetric) geometries. The pre-edge peak at 3 eV arises from a dipole forbidden but quatrupole allowed transition $1s \rightarrow 3d$. For a centrosymmetric geometry, this feature is very weak. When the 3d orbital is mixed with the $4p$ component in a non-centrosymmetric geometry, such as a square pyramid, the $1s \rightarrow 3d$ transition becomes slightly allowed, resulting in the pre-edge peak seen at 3 eV in the spectrum of the ground state of **2**.

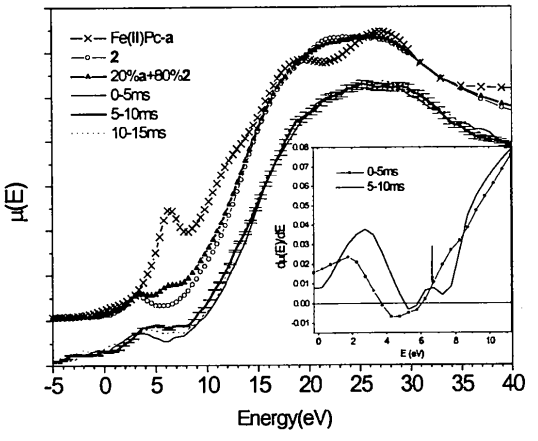

Figure 3
Top: XANES spectra of Fe(II)Pc, the ground state of **2** taken at a conventional XAFS beamline, and a linear combination of 20% Fe(II)Pc and 80% ground state **2**. Bottom: **2** at different detection times after the laser pulse. The spectrum during 0-5 ms was considered the reference spectrum before the reduction of Fe (see text). The error bars of the measured curves are indicated on the 5-10 ms spectrum. The inset shows the smoothed first derivative of the XANES spectrum of **2** at two different times. The appearance of a "bump" similar to that of Fe(II)Pc is evidenced by the peak at 6.2 eV.

The oxidation state and the ligation state of Fe in **2** are both likely to change upon photoinduced ET. Although the transient optical absorption results indicated possible reduction of Fe(III) to Fe(II), the ligation state can be either unchanged, reduced to four coordinate square planar, or increased to six-coordinate octahedral geometry. The XANES spectrum **2** at 5-10 ms (the ground state mixed with the optimal concentration of a charge separate intermediate generated by the laser pulse) in Figure 3 can be best fit by a reconstructed spectrum using 20% of Fe(II)Pc and 80% of the ground state **2**. The down-shift of the edge energy in the spectrum of **2** at 5-10 ms from that of **2** at 0-5 ms in the region of 8-15 eV is comparable to the down-shift of the edge in the reconstructed spectrum from that of the ground state **2**. Moreover, the first derivative of the spectrum for **2** at 5-10 ms shows a turn towards zero at 6.2 eV where the sharp peak in the XANES of the square planar Fe is located. However, a better signal/noise ratio may be needed to confirm this. Therefore, the apparent up-shift of the pre-edge feature is due to the characteristic peak at 6.2 eV for the square planar geometry. These changes in XANES spectra suggest a geometry where the bond between the pyridine ligand and the Fe in the intermediate ZnP^+-py-spacer-Fe(II)P-py has been broken or substantially weakened. Evidence for the square planar geometry around the Fe atom in the ZnP^+-py-spacer-Fe(II)P-py intermediate indicates that the ligand may serve to gate the ET. When pyridine binds to Fe(III), the reduction to Fe(II) is energetically more favorable. However, once the electron is transferred to Fe(III)P-py, breaking the Fe-pyridine bond makes back electron transfer to the ground state more difficult. Thus, the combined optical and X-ray results indicate that pyridine ligation enables ET both into and out of the iron porphyrin, while dissociation of the ligand hinders these processes.

This work was supported by the Division of Chemical Sciences, Office of Basic Energy Sciences, Department of Energy under contract W-31-109-ENG-38. We thank Dr. Pedro A. Montano for his constant support.

REFERENCES

Barbara, P. F., Meyer, T. J. & Ratner, M. A. (1996). *J. Phys. Chem.* **100,** 13148-13168.

Bianconi, A., Cogiu-Castellano, A., Durham, P. J., Hasnain, S. S. & Phillips, S. (1986). *Nature* **318,** 685-687.

Cartier, C., Monenteau, M., Dartyge, E., Fontaine, A., Tourillon, G., Michalowicz, A. & Verdaguer, M. (1992). *J. Chem. Soc. Dalton Trans.* 609-618.

Chance, B., Fischetti, R. & Powers, L. (1983). *Biochemistry* **22,** 3820-3829.

Chen, L. X., Bowman, M. K., Montano, P. A. & Norris, J. R. (1993). *J. Am. Chem. Soc.* **115,** 4373-4374.

Chen, L. X., Bowman, M. K., Wang, Z., Montano, P. A. & Norris, J. R. (1994). *J. Phys. Chem.* **98,** 9457-9464.

Chen, L. X., Wang, Z., Burdett, J. K., Montano, P. A. & Norris, J. R. (1995). *J. Phys. Chem.* **99,** 7958-7964.

Fontaine, A., Baudelet, F., Dartyge, E., Guay, D., Itie, J. P., Polian, A., Tolentino, H. & Tourillon, G., (1992). *Rev. Sci. Instrum.* **63,** 960-965.

Lee, P. L., Beno, M. A., Jennings, G., Ramanathan, M., Knapp, G. S., Huang, K., Bai, J. & Montano, P. A. (1996). *Rev. Sci. Instrum.* **65,** 1-6.

Natan, M. J., Baxter, W. W., Kuila, D., Gingrich, D. J., Martin, G. S. & Hoffman, B. M. (1991). *Adv. Chem. Ser.* **228,** 201-213.

Nocek, J. M., Sishta, B. P., Casey, J. R., Mauk, A. G. & Hoffman, B. M. (1997). *J. Am. Chem. Soc.*, **119,** 2146-2155.

Perman, B., Srajer, V., Ren, Z., Teng, T-Y., Pradervand, C., Ursby, T., Bourgeois, D., Schotte, F., Wulff, M., Kort, R., Hellingwerf, K. & Moffat, K. (1998). *Science* **279,** 1946-1950.

Powers, L., Sessler, J. L., Woolery, G. L. & Chance, B. (1984). *Biochemistry* **23,** 5519-5523.

Smith, T. A., Penner-Hahn, J. E., Berdin, M. A., Doniach, S. & Hodgson, K. O. (1985). *J. Am. Chem. Soc.* **107,** 5945-5955.

Thiel, D. J., Livins, P., Stern, E. A. & Lewis, A. (1993). *Nature* **362,** 40-43.

Wiederrecht, G. P., Niemczyk, M. P., Svec, W. A. & Wasielewski, M. R. (1996). *J. Am. Chem. Soc.* **118,** 81-88.

(Received 10 August 1998; accepted 11 November 1998)